Ground-based observation of molecular clusters and nucleation mode particles in the Amazon

Deleted: Direct

Daniela Wimmer[1], Stephany Buenrostro Mazon[1], Hanna Elina Manninen[1,2], Juha Kangasluoma[1], Alessandro Franchin[1,3,4], Tuomo Nieminen[1,5], John Backman[6], Jian Wang[8], Chongai Kuang[8], Radovan Krejci[7], Joel Brito[9,10], Fernando Goncalves Morais[9], Scot Turnbull Martin[11], Paulo Artaxo[9], Markku Kulmala[1], Veli-Matti Kerminen[1] and Tuukka Petäjä[1]

[1]Department of Physics, University of Helsinki, Gustaf Hallströmin katu 2a, 00560, Helsinki, Finland
[2]European Organization for Nuclear Research (CERN), 1211 Geneva, Switzerland
[3]NOAA Earth System Research Laboratory (ESRL), Chemical Sciences Division, Boulder, CO, USA
[4] Cooperative Institute for Research in Environmental Sciences, University of Colorado Boulder, Boulder, CO, USA
[5]Department of Applied Physics, University of Eastern Finland, Post Office Box 1627, 70211 Kuopio, Finland
[6]Finnish Meteorological Institute, Atmospheric composition research, Erik Palménin aukio 1, 00560, Helsinki, Finland
[7]Stockholm University, Department of Environmental Science and Analytical Chemistry (ACES), 106 91 Stockholm, Sweden
[8]Environmental and Climate Sciences Department, Brookhaven National Laboratory, Upton, New York, USA
[9]Institute of Physics, University of São Paulo, de Fisica, Universidade de Sao Paulo, Rua do Matao 1371, CEP 05508-090, Sao Paulo, Brazil
[10]Laboratory for Meteorological Physics (LaMP), Université Clermont Auvergne, F-63000 Clermont-Ferrand, France
[11]School of Engineering and Applied Sciences, Harvard University Cambridge, Massachusetts 02138, United States of America

Correspondence to: Daniela Wimmer (daniela.wimmer@helsinki.fi)

Keywords: atmospheric ions, particle formation, rainforest, high-frequency rainfall

Abstract

We investigated atmospheric new particle formation (NPF) in the Amazon rainforest using direct measurement methods. The occurrence of NPF on ground level in the Amazon region has not been observed previously in pristine conditions. In this work, pristine refers to CCN concentrations of a few hundred cm^{-3}. Our measurements extended to two field sites and two tropical seasons (wet and dry). We measured the variability of air ion concentrations (0.8–20 nm) with an ion spectrometer between 2011 and 2014 at the T0t site and between February and October 2014 at the GoAmazon 2014/5 T3 site. The T0t site is surrounded by dense rainforest, mostly unaffected by the Manaus pollution plume. The T3 site, instead is an open pasture site, 70km downwind of Manaus.

The main difference between the two sites is their geographical location. Both sites are influenced by the Manaus pollution plume yet with different frequencies. T0t is influenced by pollution about once per week, where T3 on the other hand is reached once per day/once per every second day, especially in the afternoon (Martin et al., 2010b supplementary material, Thalmann et al, 2017, de Sa et al, 2017). The sampling was performed at ground level at both sites. At T0t the instrumentation was located inside the rainforest, whereas the T3 site was an open pasture site. T0t site is mostly parallel wind to Manaus, whereas T3 site is downwind of Manaus. No NPF events were observed inside the rainforest (site T0t) at ground level during the period Sep 2011- Jan 2014. However, rain-induced ion and particle bursts (hereafter, “rain events”) occurred frequently (306/529 days) at T0t throughout the year but most frequently between January and April (wet season). Rain events increased nucleation mode (2-20 nm) particle and ion concentrations on the order of 10^4 cm^{-3}.

Deleted: We measured the variability of air ion concentrations (0.8–20 nm) with an ion spectrometer between 2011 and 2014 at the T0t site and between February and October 2014 at the GoAmazon 2014/5 T3 site.

Deleted: T0t is reached by the pollution about 1 day in 7, where the T3 site is about 15% of the time affected by Manaus.

Deleted: canopy

We observed 8 NPF events at the pasture site during the wet season. We calculated the growth rates (GR) and formation rates of neutral particles and ions for the size ranges 2-3 nm, 3-7 nm and 7-20 nm using the ion spectrometer data. One explanation for the absence of new particle formation events at the T0t site could be a combination of cleaner air masses and the rainforest canopy acting as an ‘umbrella’, hindering the mixing of the air masses down to the measurement height. Neutral particle growth rates in the 3-7 nm regime showed two phenomena. Growth rates were either about 2 nmh^{-1} or about 14 nmh^{-1}. There was no clear difference in the sulfuric acid concentrations for NPF event days vs days without NPF. The two major differences between NPF days and non event days are two. A factor of 2 lower condensation sink on NPF days and different air mass origins for the NPF days compared to non event days.

Deleted: Back trajectory calculations show different

Deleted: NPF

1 Introduction

Globally, atmospheric new particle formation (NPF) and growth has been estimated to account for a major, if not dominant, fraction of atmospheric cloud condensation nuclei (Merikanto et al. 2009, Wang and Penner, 2009, Yu and Luo, 2009, Dunne et al., 2016; Kulmala et al., 2016). The formation of atmospheric nanoparticles is a multi-stage process, in which stable clusters form from gas phase precursors followed by the activation of these clusters and further growth (Kulmala et al. 2014). Although atmospheric NPF is occurring frequently in many environments (e.g. Kulmala et al. 2004, Manninen et al. 2010), the Amazon basin is one of the locations where the initial steps of the formation of nanoparticles have not been previously observed from ground based measurements (Martin et al, 2010a). In the Amazon, emissions and oxidation of volatile organic compounds (e.g. Lelieveld et al. 2008), aerosol activation to cloud droplets, and eventually rain formation, are tightly connected to synoptic processes, such as deep convection for example (Lelieveld et al. 2008, Wang et al., 2016). Aerosol concentrations in the atmosphere are rapidly changing with deforestation and the associated biomass burning and economic development in the Amazon region (Martin et al. 2016, Artaxo et al., 2013).

Deleted: for

Deleted: and interlinked with meteorological processes

Deleted: the boundary layer development and

The Manaus metropolis (population 2 million) is the capital of the state of Amazonia, Brazil, surrounded by the largest rainforest on Earth, as shown in Fig 1 (Martin et al, 2017). The measurements discussed in this paper took place at two different locations in the Amazon rainforest: a pasture site 70 km downwind from Manaus (T3; Martin et al., 2016), and a site inside the rainforest, mostly unaffected by Manaus pollution (T0t; Martin et al., 2010b). The sites will be described in more detail in section 2.1. Depending on the wind direction, these sites can represent (i) one of the most natural continental locations on Earth, or (ii) a location affected by both polluted metropolis and rainforest (Martin et al., 2016). The different meteorological and aerosol dynamical conditions during the wet and the dry season in the Amazon basin, offer an interesting natural environment for studying aerosol particle dynamics. During most of the wet season the Amazon basin is one of the cleanest continental regions on Earth (Andreae, 2007; Martin et al., 2010a, Artaxo et al., 2013, Andreae et al., 2015). During the dry season, the Amazon basin is highly influenced by anthropogenic emissions mostly from biomass burning. Additionally, our study region experiences frequent high-intensity precipitation episodes.

Deleted: clearing

Deleted: canopy

Deleted: The regular synoptic changes between the wet and dry seasons offered an additional important scientific contrast to study aerosol dynamics.

Deleted: , while

Deleted: during

Deleted: and local fire emissions are ubiquitous throughout the basin

The primary goal of this paper was to investigate the occurrence of new particle formation (NPF) and growth in the Amazon region, and to quantify the role of ions and aerosol particles in this process. No NPF events were observed during the long-term measurements at the site largely unaffected by Manaus emissions. A clear correlation between rain intensities and ion concentrations was found for both measurement sites. At the more polluted pasture site, we observed 8 NPF events, which occurred during the wet season. The data from comprehensive measurements shows that the freshly formed particles were growing to sizes of about 60 nm at which they start to act as cloud condensation nuclei.

2 Methods

The measurements discussed here were conducted in 2014 outside the rainforest canopy as a part of the Green Ocean Amazon (GoAmazon2014/5) Experiment (Martin et al., 2016), which was going on for the period from 1 January 2014 to 31 December 2015. GoAmazon2014/5 was designed to study the perturbation in cloud and aerosol dynamics by the Manaus emissions. Our measurement campaign took place during 28 January – 13 October 2014 near the city of Manacapuru, Brazil, 70 km downwind of Manaus. We compare the campaign data to long-term measurements made between September 2011 and January 2014. Wet and dry season in the Amazon are Dec-March and June-September respectively (Martin et al, 2010a). Due to the measurement periods available for our dataset, we define the dry season as dry and transition season Apr-Oct.

2.1. Measurement sites

2.1.1 Measurements inside the rainforest

The T0t ecological reserve (Martin et al, 2010b) is a terrestrial ecosystem science measurement site located 60 km north of the Manaus metropolis in the central region of Brazil (-2.609° lat, -60.2092° lon). Manaus is the capital of the state of Amazonia, Brazil and is located where the Rio Negro merges with the Solimoes river which then form the Amazon river. The city with more than 2 million inhabitants is the seventh biggest city in Brazil and is surrounded by 1500 km of forests in all directions (IBGE, 2015; Martin et al., 2016). T0t is mostly unaffected by the Manaus pollution and is surrounded by dense rainforest. It allows the characterization of an almost completely undisturbed natural environment (Martin et al, 2016). The rainforest canopy is homogeneous with an average height of 30 m. A Neutral cluster and Air Ion Spectrometer (NAIS) was placed inside a hut within the rainforest canopy, with an inlet system 2 m above the ground level. In addition to the ion spectrometer measurements, the measurement hut hosts a Vaisala system (WXT520) for acquiring meteorological parameters and a differential mobility particle sizer (DMPS). The DMPS was sampling from an inlet 60 m above the ground level, therefore sampling aerosols above the canopy. Both the DMPS and the NAIS were measuring at the T0t site from 2011-2014. For the GoAmazon2014/5 campaign the

Deleted: Inside canopy measurements

Deleted: S

Deleted: W

Deleted: Manaus is situated at the confluence of the Black River (Rio Negro) with the Solimões river, which together form the Amazon river. The city is an isolated urban region with a population of more than 2 million people (IBGE, 2015; Martin et al., 2017)

Deleted: it

NAIS was moved to a measurement site outside the rainforest canopy, which is described in Section 2.1.2. The nucleation and growth rates reported here were all determined from the direct measurements provided by the NAIS.

2.1.2 Measurements outside the rainforest

T3 is a site equipped with an Atmospheric Radiation Measurement (ARM) Climate Research Facility of the United States Department of Energy, 70 km downwind of the city of Manaus (-3.2133° lat, -60.5987° lon; Mather et al., 2014) and included an ARM Mobile Aerosol Observing System (MAOS). The site is an open pasture site, where the Manaus pollution plume regularly intersects and the rainforest canopy did not hinder mixing. Due to the site location, T3 is either a pristine environment or highly influenced by the Manaus pollution plume, mainly depending on the wind direction. This site also hosted numerous instrument systems from other GoAmazon2014/5 participants (Martin et al., 2016). The same NAIS used at T0t was deployed at T3 from end of January 2014 onwards. Sub-3 nm neutral particle measurements were done with a Particle Size Magnifier (PSM). The PSM and NAIS inlets sampled at 2 meters from ground level.

2.2 Instrumentation

2.2.1 Neutral cluster and Air Ion Spectrometer (NAIS)

A Neutral cluster and Air Ion Spectrometer (NAIS; Manninen et al., 2016) was used to determine the early stages of atmospheric nucleation and subsequent growth. The NAIS measures the mobility distributions in the range 3.2–0.0013 cm^{2}V^{-1} s^{-1}, which corresponds to a mobility diameter range of 0.8–42 nm. The ion and particle size distributions are measured in three different stages: ion, particle and offset. The NAIS consists of two parallel cylindrical DMA's (Differential Mobility Analyzers), one for classifying negative ions and the other for positive ions. When in ion mode, corona chargers and electrostatic filters are switched off to allow only naturally charged ions into the DMA. During the neutral particle mode, the particles are charged and then filtered by an electrostatic filter to neutralize them before entering the DMA. The inlet flow into the NAIS is 60 liters per minute (LPM), whereas the sample and the sheath flows of the DMA's are 30 and 60 LPM, respectively. The NAIS time resolution was set to 5 min, where a measurement cycle of negative ions, positive ions, and total particles is included.

Deleted: **Outside canopy**

Deleted: **measurements**

Deleted: S

Deleted: W

Deleted: located in a pristine environment

Deleted: Under the day-to-day variability in the meteorology, both clean and polluted air masses, mixed to variable degrees, arrived at T3

Deleted: The site is located in a clearing of the rainforest where the canopy did not hinder mixing.

Deleted: in an open clearing

The instrument and calibration are described in more details in Asmi et al. (2009), Wagner et al. (2016) and Manninen et al. (2016). The accuracy of the ion concentration of the NAIS was estimated to be 10-30%, which was mainly due to flow rate uncertainties (Manninen et al., 2016; Wagner et al., 2016). During the campaign, the deposition of particulate matter inside the instrument caused decreasing flow rates between the maintenance periods. This may have further increased the uncertainty in measured particle sizes and number especially at sizes bigger than 20 nm.

2.2.2 Particle Size Magnifier (PSM)

The instrument we used to determine aerosol particle concentrations at sizes below 3 nm was a Particle Size Magnifier (PSM; Airmodus A09; Vanhanen et al., 2011). The PSM is a mixing-type condensation particle counter (CPC), in which the aerosol is turbulently mixed with air saturated with diethylene glycol (DEG). DEG only grows the particles to about 90 nm, so the PSM system consists of a second stage, where the particles are grown to optically detectable sizes. The 50% activation diameter of the instrument can be varied in size range 1–4 nm in mobility diameter (Vanhanen et al., 2011) by changing the mixing ratio of the saturator and sample flows. At GoAmazon2014/5, the PSM was used in scanning mode. In scanning mode, the saturator flow is continuously changing, altering the cut-off diameters from 1-4 nm. One scan takes 4 min and the system was setup to do one upscan, followed by a downscan. Due to the challenging measurement conditions, the size resolved data could not be used for the analysis.

Prior to the deployment during the GoAmazon2014/5 campaign, the PSM was equipped with an inlet system, especially designed to decrease the relative humidity of the sample without disturbing the sample itself and maintaining high flow rates (10 Lpm) until the actual sampling to minimize diffusion losses. The inlet system consists of a core sampling probe combined with a sintered tube. The core sampling probe consists of two cylindrical tubes with different outer diameters (10 mm and 6 mmm). The larger diameter of the outer tube allows up to 10 Lpm total laminar flowrate, to minimize diffusional losses. The inner tube is directly attached to the PSM with an airflow of 2.5 Lpm. The excess airflow is discarded into an exhaust line (Kangasluoma et al, 2016). Downstream of the core sampling line is a sintered tube where dry pressurized air is introduced. The water molecules in the sample flow are pushed towards the outer walls of the sinter material by diffusion, drying the airflow.

Laboratory studies have shown that the RH affects the counting efficiency of the PSM drastically (higher sensitivity at smaller sizes at higher RH; Kangasluoma et al, 2013, Iida et al, 2009). The PSM with the inlet was calibrated, using limonene and its oxidation products (Kangasluoma et al, 2014) as the test aerosol. We expect the aerosol sample in Brazil to be mostly organic species, hence the decision to calibrate with limonene. The resulting lowest cut-off diameter of the PSM was 1.5 nm (±0.3 nm). The estimated error is a combination of calibration uncertainty and the influence of the ambient RH on the cut-off diameter of the PSM. To our knowledge, this is the first time when results from ground-based sub-3 nm aerosol particle measurements are shown for the Amazon rainforest. In total, 38 days of data obtained during the dry season were used.

2.2.3 Supporting instrumentation at T0t site

Submicron aerosol number size distributions and total particle number concentrations were monitored with a DMPS system (Aalto et al., 2001) and a CPC. The time resolution of the CPC with a cut-off of about 6 nm was 1 minute. The DMPS measured number size distributions over the mobility diameter range of 6–800 nm (Backman et al., 2012). The complete size distribution is obtained in a 10-minute time resolution. The DMPS system was designed so that the size segregated aerosols were measured for 8 minutes and for the remaining 2 minutes of the 10 min cycle, total particle number concentrations were measured with the CPC directly using a bypass valve. The line losses for the DMPS were estimated to be about 50% for particles smaller than 4 nm in diameter during the AMAZE-08 Experiment (Martin et al., 2010b). For the measurements reported here, a similar setup with a 60 m sampling line was used. The DMPS data reported here are qualitative, not quantitative, as the losses due to diffusion in the sampling line are not precisely known and therefore not taken into account in the data presented later in this manuscript. Formation and growth rates were analyzed using NAIS data only. Meteorological data from a Vaisala weather station includes temperature, relative humidity, wind speed and wind direction, and precipitation intensity.

Deleted: for a similar setup

Deleted: included

2.3 Measurement periods: wet and dry season

The differences in tropical seasons - the wet and dry seasons - allowed for an additional comparison between two contrasting environmental conditions (Martin et al., 2016, Artaxo et

Deleted: changes between

Deleted: -

Deleted: offered

al., 2013). The aerosol particle population in the Amazon basin is a mixture between pristine conditions and anthropogenic influence, which is mostly dominated by biomass burning emissions. Biomass burning emissions are strongest during the dry and transition season (April to October), whereas in the wet season (December to March), the Manaus plume aside, the Amazon basin is one of the cleanest continental regions on Earth (Andreae, 2007; Martin et al., 2010a). The most intense biomass burning and atmospheric perturbations take place at the southern and eastern edges of the forest (Brito et al., 2014), however their transport impact the whole basin. During the dry season, the wet deposition decreases whereas the condensation sink increases. That leads to an overall increase in aerosol concentration in the accumulation mode of about one order of magnitude even in remote areas (Artaxo et al., 2013).

Deleted: in dynamic balance with the ecosystem and anthropogenic contributions (e.g. biomass burning; which produces them directly and indirectly) and the hydrological cycle (which removes them).

Deleted: In

Deleted: In the dry and transition season (April to September), biomass burning emissions are prevalent throughout the basin.

Deleted: Wet

Deleted: increases during the dry season

Planetary boundary layer development has also a seasonal behavior: stable nocturnal layer and a strong vertical mixing during daytime. The vertical mixing can be enhanced during the wet season as particles are lifted out of the mixed layer due to convective clouds. The nocturnal layer on the other hand traps the emissions near the surface, which can be more pronounced during dry season, as biomass burning usually starts at midday and continues into evening hours (Martin et al, 2010a). The boundary layer development is also different at the two different measurement sites. It develops more rapidly in the pasture area, causing a more efficient vertical mixing compared to the site enclosed by rainforest. From our observations, we conclude that the main differences in the dynamics of the aerosol particle population at the two measurement sites is due to the ‘umbrella effect’ of the rainforest canopy.

Deleted: due to

2.4 Data analysis

All the available data from the NAIS was cleaned for potential instrumental noise. The cleaning process was done visually using the particle and ion size distributions as surface plots. The NAIS can measure both naturally charged ions and neutral particle size distributions. We present data from both measurements in the following. Based on this initial screening, the decision was made whether one or more of the electrometers was reliable or not and the non-reliable data was removed. On 44.7% of the days the cleaning procedure was applied. Mostly the particle data in the smaller size ranges (up to 3 nm) was unreliable. The procedure follows the guidelines introduced by Manninen et al., 2010. We observed an unexplained increase in the concentrations of the cluster ions in the NAIS towards the end of October 2013 to January 2014 at the T0t site. This increased level continued when the NAIS was taken to the T3 site. We consider this drift instrumental. By comparing the 2014 concentrations of the NAIS channels to those prior to the increase (January 2012 and 2013), a correction factor of 1.8 was applied to the 4 smallest size channels of the NAIS (0.8-1.25 nm) to account for the drift for the subsequent data.

Deleted: first

Deleted: channels

Rain-induced ion events were selected as a day which included an ion burst coincided with the onset of precipitation. Median and maximum (95 percentile) ion concentrations were calculated during the time when the rain intensity was >0 mm hr^{-1} (>0.1 mm hr^{-1} for the T3 site, as the rain data from the T3 site showed some rain signal on almost all of the days). In some of the days, rain occurred sporadically several times per day. In order to take this into account, two separate rain events were classified as such if they occurred >1 hr. apart from the end of the first and the start of the second. Any fluctuations in the rain intensity for a shorter time period than 1 hr was considered to be part of a single rain event.

The new particle formation event analysis from the ion spectrometer data, including the event classification and formation and growth rate calculations, followed the already well-defined guidelines (Kulmala et al., 2012). In the data analysis, the first step was to classify all available days into NPF event and non-event days according to methods introduced earlier by Hirsikko et al. (2007) and Manninen et al. (2010). The days which do not fulfill the criteria of an event or non-event day, are categorized as undefined days. However, no days were classified as undefined days in this study. The classification was done visually using daily contour plots of particle number size distributions. The second step in the analysis was to calculate various quantities related to each NPF event, such as the particle growth rate (GR) and formation rate (J). Both growth and formation rates were calculated for three different size bins (2-3 nm, 3-7 nm and 7- 20 nm in diameter) using both ion and neutral particle data from the NAIS. The particle growth rate was determined by finding the times at which the maximum concentrations of ions/particles in each of these size bins occurred. A fit between the points was then applied to determine the GR. The particle formation rate was determined for lower end of each size bin (2, 3 and 7 nm) by taking into account the growth rates, condensation sink and coagulation sink.

3 Results

All the times mentioned below are local Manaus time (LT), which is Coordinated Universal Time (UTC) –4 h.

3.1 Number concentrations of ions and particles at the two sites

An overview of the observed number concentrations of ions and particles as well as ambient conditions at the two measurement sites is presented in Table 1. We divided the measured ions into three sub-size ranges: cluster ions (0.8-2 nm), intermediate ions (2-4 nm) and large ions (4-20 nm) and the same for neutral particles. The lower and upper limits of the intermediate ion size range vary in the scientific literature (see Hirsikko et al., 2011 and references therein). Here, 2-4 nm was chosen, as this size range seems to work well in differentiating between atmospheric new particle events and non-events when using ion measurements (Leino et al., 2016). Additionally, the wet and dry seasonality characteristic for the Amazon (Rissler et al. 2006, Martin et al. 2010a) can be observed in the concentration of the large ions (4-20nm): the local biomass burning during the dry season seems to increase large ion concentrations, whereas during the wet season their concentrations are decreased most likely due to wet deposition and reduced source strengths.

Deleted: is expected

Deleted: expected to

Particle and ion concentrations were, in general, higher at the open pasture T3 site, downwind of Manaus. The average concentrations of 4 – 20 nm particles were up to a factor of 3 higher in comparison to the less polluted site (T0t). The environmental variables were relatively similar between the two sites, the temperature and RH being slightly lower at the pasture site compared with the inside rainforest site.

Deleted: parallelwind of Manaus and

Deleted: inside the canopy

Deleted: outside canopy

Deleted: canopy

3.1.1 Inside rainforest site (T0t)

Deleted: **canopy**

Figure 2 shows the monthly variability of particles in two size ranges (0.8-2nm, 2-4 nm) for the 2011-2014 period. The cluster ions had a median concentration of 814 cm^{-3} and 968 cm^{-3} (wet) and 605 cm^{-3} and 765cm^{-3} (dry) for negative and positive ions, respectively. These medians are higher than those found in several other locations (eg. urban Paris, Dos Santos et al. 2015; coastal Mace Head, Vana et al. 2008 and Finokalia, Kalvitis et al. 2012; Puy de Dome, Rose et al. 2016), but comparable to those reported at a boreal forest site in Hyytiälä, Finland (Hirsikko et al. 2005). Higher cluster ion concentrations have been reported in an Australian rainforest in Tumbarumba (Suni et al. 2008) and in a wetland site in Abisko (Svennigsson et al., 2008), both sites having concentrations of ~2400 (1700) cm^{-3} for negative (positive) ions. The size bin of 2-4 nm had a median concentration of 5–11 cm^{-3} for both negative and positive ions. Large ions 4–20 nm had a median negative (positive) ion concentration of 84 (147) cm^{-3}

Deleted: seasonal

Deleted: ions and

Deleted: the three size

Deleted: and 4-20 nm

Deleted: 723

Deleted: 879

Formatted: Superscript

Formatted: Superscript

Deleted: 10

Deleted: 5

Deleted: 153

(wet) and 132 (162) cm^{-3} (dry) when considering the 149 days (out of 524 days), that had data for this size range. These values are comparable, for example, to intermediate and large ion concentrations found in coastal Mace Head (Vana et al. 2008) outside the periods of rain or active NPF. In general, the positive cluster ion concentrations are higher in all the cluster ion and intermediate ion size classes for all the months. Table 2 summarizes the annual concentrations of ions and total particles for the three size bins.

Differences between the wet (Dec-Mar) and dry and transition season (Apr-Oct) were also observed in the diel cycle of the ion and particle concentration. Positive and negative cluster ion concentrations were, on average, higher during the wet season compared to the dry season as shown in Table 1.

The total concentrations of 2-4 nm and 4-20 nm neutral particles had similar daytime peaks with otherwise stable night-time concentrations (Fig. 3). The median concentration of 2-4 nm neutral particles was ~500 cm^{-3}, which about a factor 100 higher than the median concentration of 2-4 nm ions. Similar to ions in the same size range, 4-20 nm particles peaked at around midday, reaching values of about 1000 to 2000 cm^{-3}.

3.1.2. Outside rainforest site (T3)

The median ion and particle number concentrations during the wet and dry season at the T3 site, outside the canopy and downwind of Manaus, are given in Table 1. The diel cycles of ion and neutral particle concentrations at this site appeared to be very similar in both wet and dry season. The cluster ions showed a clear 24 hr cycle: in the mornings (00:00-07:00) their concentrations were ~1500 cm^{-3} for negative ions, then decreased to ~1000 cm^{-3} and eventually increased back to ~1500 cm^{-3} after 18:00. This daytime decrease in the concentration is most likely due to the dilution of the boundary layer. The intermediate ions (2-4 nm) showed higher concentrations between 03:00 and 06:00 during the dry season compared with the wet season.

The total particle concentration measured by the MAOS CPC (>10 nm total particle concentration) did not show any diel seasonal cycle. The median total particle concentrations were about a factor of 1.5 higher during wet season (about 1000 cm^{-3}) compared with the dry season (about 700 cm^{-3}).

3.2 Rain-induced ion formation events at inside rainforest measurement site

Formatted: Superscript

Deleted: Cluster ion concentrations are clearly higher in Oct-Dec for both seasons.

Deleted: In both seasons, there were more positive than negative cluster ions (Table 1). The lower concentrations of negative ions are expected due to the Earth's ground 'electrode' effect, in which negative ions are pushed away from the Earth surface (Hoppel W. A., 1967). Additionally, cluster ions (0.8-2 nm) showed slightly higher concentrations in the morning and evening, compared to other times of the day. Enhanced median cluster ion concentrations in the early morning have also been reported elsewhere, likely due to higher radon concentration levels at that time of the day (Hirsikko et al 2011 and references therein). A dip in the median ion concentration after midday coincides with a higher median concentration of large ions, which is a sign of a larger sink for cluster ions. Intermediate and large ions (2-4nm and 4-20 nm) had only one daytime peak in their concentration in both seasons, similar to the total particle concentrations shown in Figure 3. For 2–4 nm ions, this occurred in the late afternoon and was more pronounced during the wet season compared with the dry season for both polarities. The peak does not seem to be a result of the wet season's rain-induced ion bursts (Horrak et al. 1998), as discussed in more detail in Section 3.2. Lastly, 4-20 nm ions peaked at around midday during the wet season, while their diel pattern was more irregular during the dry season. The negative 4-20 nm ions had the highest concentrations (>1000 cm^{-3}) during the dry season, most likely due to biomass burning and weaker wet deposition. This feature could not be observed for positive large ions.

Deleted: **canopy**

Deleted: two

Deleted: dry

Deleted: 5

Deleted: wet

Deleted: **canopy**

While no NPF events were observed inside the rainforest site (site T0t), rain-induced ion burst events (hereafter, rain-events) were common and observed during 306 out the 524 measurement days. Since multiple rain episodes could occur in a single day, each rain event was investigated separately, giving a total of 579 rain-events. Figure 4 shows an example of multiple rain-events that took place during 24 January 2013 (wet season). It is clear from this Figure that the negative ions in the size ranges of 1-3 nm and 3-7 nm increased during the precipitation. A similar feature for 2-8 nm negative ions during rain events has also been reported for an Australian rainforest (Suni et al. 2008). Positive ions increased only in the 3-7 nm size range, and showed even a decrease in the 1-3 nm size range during the time of the precipitation.

Deleted: canopy

Rain-induced bursts are likely a result of a balloelectric effect, in which splashing water produces intermediate ions such that the negative ions are smaller in size than the positive ions (Horrak et al., 2005, Hirsikko et al., 2007, Tammet et al., 2009). The duration of the 579 rain events varied from a couple of minutes to 22 hours, with over half the rain events lasting for two hours or less. The rain events were more common during the wet season, peaking in August which can be considered as transition season (Fig. 5) when also the median rain intensity was higher. Although less frequent, rain-induced particle bursts were also observed during the dry season. Wang et al., 2016 reported the production of small aerosol particles, as a result of new particle formation at cloud outflow regions and further transport into the boundary via strong convection during precipitation events in the Amazon. In the study by Wang et al. the <20 nm particle concentrations decrease very rapidly, therefore we suggest the process that we observe to be a local one, as described above. Also, the production of ions we observed only lasted for the duration of the precipitation, whereas Wang et al., observed a change in the size spectrum that lasted for hours even after the precipitation event.

Figure 6 shows the correlation between the median ion concentration and rain intensity during each rain event. While no clear correlation between these two quantities was found, some specific features were apparent. First, at the inside canopy site (T0t), the highest cluster ion and 2-4 ion concentrations occurred almost entirely during rather strong rain intensities. Second, at the site outside the rainforest (T3) shown in the same Figure for comparison, some log-linear relation between the ion concentration and rain intensity could be observed for rain intensities >1 mm h^{-1} for all the three size bins.

Deleted: canopy

Rain events were evident also when looking at the total particle concentrations measured by the NAIS, as depicted in Figure 7. The first rain event showed a maximum of about 40 mmh^{-1} and the second one about 10 mmh^{-1}. In this example, the rain intensity peaks twice, the first one at ~09:00 followed by a second one at ~11:00. The ion and particle concentrations measured by the NAIS followed these two peaks closely. Additionally, the DMPS data showed an appearance of nucleation mode particles between 6 and 10 nm following the onset of rain. The DMPS was sampling at a height of 60 m, which is well above the rainforest canopy. The concentration of these 6-10 nm particles increased to ~20 cm^{-3} during the rain event, while being below 5 cm^{-3} throughout the day outside this peak. The 10-20 nm particle concentration showed first a decrease followed by a slight increase up to ~35 cm^{-3}, peaking later than the 6-10 nm particles. However, it is unlikely that these 10- 20 nm particles originate from the same rain-induced burst as seen inside the canopy, as there is no apparent particle growth from the NAIS measurements. It is unlikely that those particles survive until the top of the canopy, as the tree leaves would filter them out. Wang et al. (2016) reported that nucleation mode particles produced in cloud outflows will be transported down with the rain, such that they can be observed at the ground level as an increase in nucleation and Aitken mode concentrations (Dp <50 nm). The appearance of 6-10 nm particles with its peak concentration, could present a similar scenario of small particles brought down from the free troposphere.

3.3 New particle formation events at T3

Table 3 summarizes the overall statistics collected at the pasture site (T3). We observed no NPF events during the dry season, while on 12% of the days during the wet season we did observe NPF. Similar event frequency has been observed in Finnish boreal forest environment during autumn for example (Kontkanen et al., 2017). An earlier study by Backman et al. (2012) showed that in metropolitan area of São Paulo (population 20 million), Brazil, NPF events occurred on 18% of the days.

From the NAIS measurements, a total of 113 days were available for the outside canopy measurements. For the wet season, the data from 28 January until 31 March were used (64 days) and for the dry season the data from 29 August until 13 October was used (46 days). Due to technical issues, no NAIS data were available for the period 1 April – 28 August 2014. The PSM measurements were carried out during the dry season only. In total, 38 days of the PSM data were used and the results are shown in Figure 8. The PSM was used in scanning mode but

Formatted: Superscript

Formatted: Superscript

Deleted: seemed to have two

Deleted: are

Deleted: , as the total particle concentrations seen by the NAIS were of the order of 10^4 cm^{-3} in the size bin of 4-20 nm

Deleted: and subsequent increase in the 6-20 nm particle concentration,

Deleted: However, any possible above-canopy source would be masked by such high rain-induced concentrations inside the canopy, and it is likely that the dense rainforest canopy would filter small particles before reaching the ground.

Deleted: outside canopy

Deleted: could

Deleted: the

due to challenging environmental conditions, only the data measured at the highest supersaturation (total particle concentration at >1.5 nm) is shown. The PSM shows a similar diel pattern as the cluster ion concentrations measured by the NAIS (see Fig. 9). We observed a higher median concentration during the early morning (03:00-06:00), a dip in this concentrations during the early afternoon (12:00-15:00), and then a higher median concentration in the evening (18:00-24:00). This could be explained by the Carnegie curve (Harrison, R. G. and Carslaw, K. S., 2003), which shows the diel variation of the ionospheric potential.

We selected all eight NPF event days to characterize the behavior of ions and aerosol particles during the particle formation bursts. A comparison of the diel cycle for particles and ions for nucleation versus no nucleation event days is shown in Figure 9. The cluster ions showed a clear diel cycle with higher concentrations in the morning and evening both for NPF and non event days. A clear increase in the concentration of the intermediate ions (2-4 nm) occurred during the NPF event days, which is due to the growth of the ions out of the cluster ion size range (0.8-2 nm). The intermediate ion concentration increased at around 09:00, suggesting an onset of the particle formation after sunrise when the boundary layer rises and mixing starts. The number concentration of 4-20 nm total particles rose within the time window (09:00-12:00) during the nucleation events, while on non NPF days these particles showed highest concentrations after the sunrise (06:00) and sunset (18:00). The total particle concentration measured by the MAOS CPC showed a clear concentration increase on NPF event days starting from 09:00, which clearly indicates that the particles had grown from the smaller sizes to >10 nm, which is the lowest detection limit of the MAOS CPC. No clear diel pattern from the MAOS CPC measurements was visible on the non event days.

Deleted: NPF

Deleted: NPF

The type of NPF events that we observed are likely of regional nature, requiring relatively homogenous air masses for at least a few hours (Vana et al., 2004, Manninen et al., 2010). The most likely explanation that no new particle formation events have been observed at the T0t site compared to the T3 site are either the lack of sources of SO_2 to form sulfuric acid in the more remote site. Another explanation might be that the sampling at the less polluted T0t site was performed within the canopy, so the mixing of the boundary layer is hindered by the presence of the rainforest canopy. The gaps, or fluctuations, in the distinct shape of NPF could be caused by some degree of heterogeneity in the measured air masses. All the NPF events occurred during daytime, starting at around 09:00. Sunrise takes place at 06:00 in the Amazon

Formatted: Subscript

basin. All the NPF events occurred during the wet season, which might be due to the lower condensation sink at this time of the year, as shown in Table 1. The median sulfuric acid concentrations as measured by a quadrupole HOx CIMS (Martin et al, 2016, supplementary material) resulted in about 9*10^5 cm^{-3} both for nucleation event days and non event days. Similar values have been reported for Finnish boreal forest measurement site in autumn, where also about 12% of the days were classified as nucleation event days (Kontkanen et al., 2017).

Back trajectory calculations using HYSPLIT (http://ready.arl.noaa.gov/hypub-bin/trajtype.pl?runtype=archive) showed a clear difference in air mass origin arriving to the measurement site between NPF and non event days. Back trajectories were calculated 24h backwards, arriving at 13:00 UTC (09:00 LT) on the NPF days at 500m a. s. l. The same calculations were performed for each day before/after an NPF day. If an NPF event occurred on two consecutive days, the day after both events was used for the non event day back trajectory calculations. On NPF days, the 50th percentile of air masses originate from about -1.6°lat, -56.5°lon and 738.9 m a. s. l. On non NPF days, the back-trajectory calculations show origin at -2.6°lat, -56.6° lon and 537.4 m a. s. l. These air masses all originate from upstream of the Amazon river, where the NPF day air mass originate from further north, which is an area with dense rainforest. The results of the back trajectory calculations are shown in Figure 10. The red line shows the median of an ensemble or the non event days and the blue line for NPF days.

Fig. 11 shows an example of a NPF event observed at the outside canopy (T3) site for MAOS SMPS and both negative ion and total particle concentration, as measured by the NAIS. The surface Figure of the SMPS clearly shows a second mode starting from the smallest channel at around 10:00. The intermediate ion concentrations showed a clear increase during this NPF event, starting at 09:00, with a continuous growth at 10:00 to the smallest size channel of the MAOS SMPS as indicated by the black line in the lowest panel of Figure 11. The same can be observed in the large particles and ions (4-20 nm) channel from the NAIS.

Table 4 shows a comparison of the median particle and ion concentrations (25th – 75th percentiles in brackets), as well as the condensation sink for the time window 09:00-12:00 between the NPF event and non-event days. Clearly, the condensation sink was lower for the NPF event days (0.001 s^{-1}) compared with the non-event days (0.003 s^{-1}). We also compared environmental variables, including the temperature, relative humidity, wind direction and precipitation. The biggest differences were the factor of 1.6 higher median concentration of

Deleted: NPF

Deleted: NPF

Deleted: NPF

Deleted: E

Deleted: S,

Deleted: E

Deleted: Nevertheless, all airmasses pass over Manaus before reaching the measurement site.

Deleted: 0

Deleted:

Deleted: The median diameter of the smallest particle mode measured by the MAOS SMPS decreased at the start of the NPF event, followed by its continuous growth up to about 60 nm.

Deleted: Large

Deleted: also showed higher concentrations during the event, but with a time delay of about 30 minutes, indicating the growth of the small clusters to bigger sizes.

Deleted: 005

intermediate (2-4 nm) ions for the event days. The environmental variables indicated that there was no precipitation during any of the classified NPF events. On two classified NPF event days, there was precipitation before or after the NPF events (starting at 06:00 and 17:00 respectively). The median RH was about the same and the median wind direction was 83° during event days compared to 105 5° during non-event days. The temperature was relatively similar between the NPF event and non-event days.

Deleted: on

Deleted: days

Deleted: , while t

Deleted: 3% lower

Deleted: 81.6

Deleted: 6

Table 5 shows the calculated GRs, particle formation rates and condensation sinks for each of the classified NPF event day. Both these quantities were determined for three different size ranges (2-3, 3-7 and 7- 20 nm), and calculated separately for the ion and particle data. The results show considerably lower ion formation rates compared with neutral particle formation rates, consistent with observations made at most other continental sites (Manninen et al., 2010; Hirsikko et al., 2011). The growth rates of particles and ions were comparable to each other and typically smaller for the 2-3 nm size range compared with the 3-7 and 7-20 nm size ranges. An increase in the particle/ion growth rate with an increasing particle size has been reported earlier in a few other sites (see Häkkinen et al., 2013, and references therein).

We observed two regimes when looking at the neutral 3-7 nm GR. On 3 days, the GR were about 2 nm h^{-1}. Those days showed sulfuric acid concentrations of about $2*10^6$ cm^{-3}. According to theoretical calculations about 10^7 cm^{-3} of sulfuric acid can account for 1 nm h^{-1} (Nieminen et al., 2010). It is most likely that other compounds are participating to the growth. The other NPF event days, showed GR of about 14 nmh^{-1} for the same 3-7 nm size range. On those days, the sulfuric acid concentration was even lower (about $6*10^5$ cm^{-3}). These GR are most likely driven by organic compounds (Tröstl et al., 2016). Tröstl et al. calculated that about 10^6-10^7 of highly oxidized organic compounds are required to explain GR of about 10 nmh^{-1}.

4 Summary and Conclusions

We performed direct observations of atmospheric new particle formation (NPF) events in the Amazon area with state-of-the-art aerosol instrumentation. The measurement campaigns were carried out at two observation sites (T0t and T3) in the vicinity of Manaus city in Brazil. One of these sites was located inside the rainforest (T0t), providing long-term (Sep 2011-Jan 2014) measurement data to complement data from a pasture site (T3).

Deleted: canopy

Deleted: outside canopy

No NPF events were observed inside the canopy during the period Sep 2011-Jan 2014. However, we observed rain-induced ion and particle burst events ("rain-events") inside the rainforest during 306 of the 529 days. Concentrations of 2-4 nm and 4-20 nm ions and total particles were enhanced by up to 3 orders of magnitude during such rain-events (~10^4-10^5 cm^{-3}). The rain events occurred throughout the year, but were most frequent during the wet season (December to March) when also the median rain intensity was the strongest. Multiple rain events could occur during the same day, totaling 579 rain events in 306 rainy days. The duration of the rain events ranged from a couple of minutes to 22 hours, but over 50% of the events lasted for <2 hours. Overall, the median positive cluster ion (0.8-2 nm) concentrations was higher than that of negative cluster ions, as can be expected from the Earth's electrode effect (Hoppel, W. A., 1967). However, during the rain-events 0.8-2 nm and 2-4 nm negative ions dominated over similar-size positive ions. Similar rain-events were found at the pasture site (T3). The production of small (0.8-2 nm) and intermediate ions (2-4 nm) during rain events reached a maximum of 10^4 cm^{-3} at the pasture site, where it was one order of magnitude higher at the T0t site. Large ion concentrations reached similar concentrations during rain events at both measurement sites.

Deleted: canopy
Deleted: cm^{-3}
Formatted: Superscript
Deleted: January
Deleted: April
Deleted: , but weaker,
Deleted: outside the rainforest canopy
Formatted: Superscript
Formatted: Superscript

Outside the rainforest, we observed a clear diel pattern in the cluster ion concentration during both wet and dry season, with higher concentrations during the morning and evening compared with other times of the day. The results from the PSM showed a very similar pattern: the median diel cycle of >1.5 nm particles showed a higher concentration in the early morning and a dip in the afternoon followed by an increase in the evening after sunset. The diel pattern was less pronounced inside the rainforest, which indicates that the rainforest canopy acts as a sink for newly formed particles and hinders vertical mixing.

Deleted: canopy
Deleted: canopy

We observed eight NPF events showing particle growth at site T3 outside the canopy during Jan-March 2014, which is during the wet season. The formation rates were considerably higher for neutral particles compared with ions during the NPF events. The growth rates of newly formed ions and particles were comparable to each other and showed a clear increase with increasing size in the sub-20 nm size range. We found two different regimes for GRs in the 3-7 nm size range. We found 3 out of 8 NPF days with GR of about 2 nm h^{-1} and 4 out of 8 NPF days with GR of about 14 nm h^{-1}. The sulfuric acid concentrations were the same for the nucleation event days and non-event days (approx. $9*10^5$ cm^{-3}). The back-trajectory calculations using HYSPLIT did not show any clear difference between days with small GR

Deleted: Jan
Deleted: Oct

compared to days with high GR. Nevertheless, a clear difference in air mass origin on NPF days compared to the same number of days without NPF was observed. Most likely the observed growth on all the NPF days is driven by highly oxidized organic compounds (Tröstl et al., 2016). The back-trajectory calculations show air mass origin over rainforest area on NPF days, vs the Amazon river on days where no NPF was observed. As shown by the SMPS, the particles grew to sizes of around 60 nm during all the NPF events, which means they are able to act as cloud condensation nuclei (McFiggans et al, 2006; Andreae and Rosenfeld, 2008; Kerminen et al. 2012). There were clear differences in median cluster and intermediate ion concentrations between the NPF event days and non-event days for the time window of 09:00-12:00. The median cluster ion concentration was lower, and the median intermediate ion concentration was higher by a factor of 1.6, during the NPF event days compared with non-event days. The condensation sink was lower during the NPF event days (0.0016) compared with non-event days (0.003). No precipitation was observed during any of the NPF events. Most likely, during the dry season the condensation sink is too high for new particle formation.

Deleted: on

Deleted: days

Acknowledgements

We acknowledge the Academy of Finland Centre of Excellence program (grant no. 272041). We acknowledge the Atmospheric Radiation Measurement (ARM) Climate Research Facility, a user facility of the United States Department of Energy, Office of Science, sponsored by the Office of Biological and Environmental Research, and support from the Atmospheric System Research (ASR) program of that office. D.W. wishes to acknowledge the Austrian Science Fund (FWF, grant no J-3951). P Artaxo acknowledges FAPESP project 2013/05014-0 and CNPq for funding. We thank field support from Alcides Ribeiro, Bruno Takeshi and Fabio Jorge. We acknowledge logistical support from the LBA Central Office, at the INPA – Instituto Nacional de Pesquisas da Amazonia.

References

Aalto, P., Hameri, K., Becker, E., Weber, R., Salm, J., Makela, J. M., Hoell, C., O'Dowd, C. D., Karlsson, H., Hansson, H. C., Vakeva, M., Koponen, I. K., Buzorius, G. and Kulmala, M., Physical characterization of aerosol particles during nucleation events, *Tellus series B – Chemical and physical meteorology*, 53:4, 344-358; DOI: 10.1034/j.1600-0889.2001.530403.x

Andreae, M. O.: Aerosols before pollution, Science, 315, 50–51, 2007.

Andreae, M. O. and Rosenfeld D.: Aerosol-cloud-precipitation interactions. Part 1. The nature and sources of cloud-active aerosols, *Earth-Science Reviews*; 89, 13-41, 2008, DOI: 10.1016/j.earscirev.2008.03.001

Andreae, M. O., Acevedo, O. C., Araùjo, A., Artaxo, P., Barbosa, C. G. G., Barbosa, H. M. J., Brito, J., Carbone, S., Chi, X., Cintra, B. B. L., da Silva, N. F., Dias, N. L., Dias- Júnior, C. Q., Ditas, F., Ditz, R., Godoi, A. F. L., Godoi, R. H. M., Heimann, M., Hoffmann, T., Kesselmeier, J., Könemann, T., Krüger, M. L., Lavric, J. V., Manzi, A. O., Lopes, A. P., Martins, D. L., Mikhailov, E. F., Moran-Zuloaga, D., Nelson, B. W., Nölscher, A. C., Santos Nogueira, D., Piedade, M. T. F., Pöhlker, C., Pöschl, U., Quesada, C. A., Rizzo, L. V., Ro, C.-U., Ruckteschler, N., Sá, L. D. A., de Oliveira Sá, M., Sales, C. B., dos Santos, R. M. N., Saturno, J., Schöngart, J., Sörgel, M., de Souza, C. M., de Souza, R. A. F., Su, H., Targhetta, N., Tóta, J., Trebs, I., Trumbore, S., van Eijck, A., Walter, D., Wang, Z., Weber, B., Williams, J., Winderlich, J., Wittmann, F., Wolff, S., and Yáñez-Serrano, A. M.: The Amazon Tall Tower Observatory (ATTO): overview of pilot measurements on ecosystem ecology, meteorology, trace gases, and aerosols, *Atmos. Chem. Phys*., 15, 10723–10776, doi:10.5194/acp-15- 10723-2015, 2015.

Artaxo, P., Rizzo, L. V., Brito, J. F., Barbosa, H. M. J., Arana, A., Sena, E. T., Cirino, G. G., Bastos, W., Martin, S. T., and Andreae, M. O.: Atmospheric aerosols in Amazonia and land use change: from natural biogenic to biomass burning conditions, *Faraday Discuss*., 165, 203–235, 2013.

Asmi, E., Sipilä, M., Manninen, H. E., Vanhanen, J., Lehtipalo, K., Gagné, S., Neitola, K., Mirme, A., Mirme, S., Tamm, E., Uin, J., Komsaare, K., Attoui, M., and Kulmala, M.: Results of the first air ion spectrometer calibration and intercomparison workshop, *Atmos. Chem. Phys.*, 9, 141-154, doi:10.5194/acp-9-141-2009, 2009.

Backman, J., Rizzo, L. V., Hakala, J., Nieminen, T., Manninen, H. E., Morais, F., Aalto, P. P., Siivola, E., Carbone, S., Hillamo, R., Artaxo, P., Virkkula, A., Petäjä, T., and Kulmala, M.: On the diurnal cycle of urban aerosols, black carbon and the occurrence of new particle formation events in springtime São Paulo, Brazil, *Atmos. Chem. Phys*., 12, 11733-11751, doi:10.5194/acp-12-11733-2012, 2012.

de Sá, S. S., Palm, B. B., Campuzano-Jost, P., Day, D. A., Newburn, M. K., Hu, W., Isaacman-VanWertz, G., Yee, L. D., Thalman, R., Brito, J., Carbone, S., Artaxo, P., Goldstein, A. H., Manzi, A. O., Souza, R. A. F., Mei, F., Shilling, J. E., Springston, S. R., Wang, J., Surratt, J. D., Alexander, M. L., Jimenez, J. L., and Martin, S. T.: Influence of urban pollution on the production of organic particulate matter from isoprene epoxydiols in central Amazonia, Atmos. Chem. Phys., 17, 6611-6629, https://doi.org/10.5194/acp-17-6611-2017, 2017

Dunne E., Gordon H., Kürten A., Almeida J., Duplissy J., Williamson C., Ortega I. K., Pringle J.K., Adamov A., Baltensperger U., Barmet P., Benduhn F., Bianchi F., Breitenlechner M., Clarke A., Curtius J., Dommen J., Donahue N. M., Ehrhart S., Flagan R. C.,Franchin A., Guida R., Hakala J., Hansel A., Heinritzi M., Jokinen T., Kangasluoma J., Kirkby J., Kulmala M., Kupc A., Lawler M. J., Lehtipalo K., Makhmutov V., Mann G., Mathot S., Merikanto J., Miettinen P., Nenes A., Onnela A., Rap A., Reddington C. L. S., Riccobono F., Richards N. D. A.,Rissanen M. P., Rondo L., Sarnela N., Schobesberger S., Sengupta K., Simon M., Sipilä M., Smith J. N., Stozkhov Y., Tomé A., Tröstl, J., Wagner P. E., Wimmer D., Winkler P. M., Worsnop D. R., Carslaw K. S., Global atmospheric particle formation from CERN CLOUD measurements, *Science,* 354: 6316, 2016.

Dos Santos, V. N., Herrmann, E., Manninen, H. E., Hussein, T., Hakala, J., Nieminen, T., Aalto, P. P., Merkel, M., Wiedensohler, A., Kulmala, M., Petaja, T. and Hameri, K., *Atmos. Chem. Phys*., 15; 23:13717-13737, DOI: 10.5194/acp-15-13717-2015, 2015.

Hakkinen, S. A. K., Manninen, H. E., Yli-Juuti, T., Merikanto, J., Kajos, M. K., Nieminen, T., D'Andrea, S. D., Asmi, A., Pierce, J. R., Kulmala, M. and Riipinen, I.: Semi-empirical parameterization of size-dependent atmospheric nanoparticle growth in continental environments, *Atmos. Chem. Phys.,* 13, 15: 7665-7682, doi: 10.5194/acp-13-7665-2013, 2013.

Harrison, R. G. and Carslaw K. S., Ion-Aerosol-cloud processes in the lower atmosphere, *Reviews of Geophysics*, 41, 3 / 1012, doi:10.1029/2002RG000114, 2003.

Hirsikko, A, Laakso, L, Horrak, U, Aalto, P. P., Kerminen, V.-M. and Kulmala, M., Annual and size dependent variation of growth rates and ion concentrations in boreal forest, *Bor Environ Res,* 10, 357-369, 2005.

Hirsikko, A., Bergman, T., Laakso, L., Dal Maso, M., Riipinen, I., Horrak, U. and Kulmala, M., Identification and classification of the formation of intermediate ions measured in boreal forest, *Atmos. Chem. Phys*., 7, 201-210, 2007.

Hirsikko, A., Nieminen, T., Gagne, S., Lehtipalo, K., Manninen, H. E., Ehn, M., Horrak, U. Kerminen, V-M., Laakso, L., McMurry, P. H., Mirme, A., Mirme, S., Petaja, T., Tammet, H., Vakkari, V., Vana, M., Kulmala, M.' Atmospheric ions and nucleation: a review of observations, Atmos. Chem. Phys., 11, 767-798, DOI: 10.5194/acp-11-767-2011, 2011.

Hoppel, W. A., Theory of the electrode effect, Journal of Atmospheric and Terrestrial Physics, Vol. 22, 1967.

Horrak, U, Salm, J and Tammet, H, Bursts of intermediate ions in atmospheric air, JOURNAL OF GEOPHYSICAL RESEARCH-ATMOSPHERES, 103: 13909-13915, DOI: 10.1029/97JD01570, 1998.

Hõrrak, U., Tammet, H., Aalto, P. P., Vana, M., Hirsikko, A., Laakso, L., and Kulmala, M.: Formation of charged particles associated with rainfall: atmospheric measurements and lab experiments, Rep. Ser. Aerosol Sci., 80, 180–185, 2006.

Iida, K., Stolzenburg, M. R., and McMurry, P. H.: Effect of Working Fluid on Sub-2 nm Particle Detection with a Laminar Flow Ultrafine Condensation Particle Counter, Aerosol Sci. Tech., 43, 81–96, 2009.

Formatted: Finnish

Kalivitis, N., Stavroulas, I., Bougiatioti, A., Kouvarakis, G., Gagné, S., Manninen, H. E., Kulmala, M., and Mihalopoulos, N.: Night-time enhanced atmospheric ion concentrations in the marine boundary layer, *Atmos. Chem. Phys*., 12, 3627-3638, doi:10.5194/acp-12-3627-2012, 2012.

Kangasluoma, J., Junninen, H., Lehtipalo, K., Mikkilä, J., Vanhanen, J., Attoui, M., Sipilä, M., Worsnop, D., Kulmala, M., and Petäjä, T.: Remarks on Ion Generation for CPC Detection Efficiency Studies in Sub-3-nm Size Range, Aerosol Sci. Tech., 47, 556–563, 2013.

Kangasluoma J., Kuang C., Wimmer D., Rissanen M. P., Lehtipalo K., Ehn M., Worsnop, D. R., Wang, J., Kulmala M. and Petäjä T., Sub-3nm particle size and composition dependent response of a nano-CPC battery, Atmos. Meas. Tech., 7, 689–700, doi:10.5194/amt-7-689-2014, 2014.

Kangasluoma, J., Franchin, A., Duplissy, J., Ahonen, L., Korhonen, F., Attoui, M., Mikkilä, J., Lehtipalo, K., Vanhanen, J., Kulmala, M., Petäjä, T. (2016). Operation of the Airmodus A11 nano Condensation Nucleus Counter at various inlet pressures, various operation temperatures and design of a new inlet system. Atmos Meas Tech 9:2977-2988.

Kerminen, V-M, Paramonov, M., Anttila, T., Riipinen, I., Fountoukis, C, Korhonen, H., Asmi, E., Laakso, L., Lihavainen, H., Swietlicki, E., Svenningsson, B., Asmi, A., Pandis, S. N, Kulmala, M. and Petaja, T., Cloud condensation nuclei production associated with atmospheric nucleation: a synthesis based on existing literature and new results, *Atmos. Chem. Phys.,* 12, 24: 12037-12059; doi: 10.5194/acp-12-12037-2012, 2012.

Kontkanen J., Lehtipalo K., Ahonen L., Kangasluoma J., Manninen H. E., Hakala J., Rose C., Sellegri K., Xiao S., Wang L., Qi X., Nie W., Ding A., Yu H., Lee S., Kerminen V.-M., Petäjä T. And Kulmala M., Measurements of sub-3 nm particles using a particle size magnifier in different environments: from clean mountain top to polluted megacities *Atmos. Chem. Phys.*, 2163–2187; doi:10.5194/acp-17-2163-2017, 2017.

Kulmala, M., Vehkamaki, H, Petaja, T., Dal Maso, M., Lauri, A, Kerminen, VM, Birmili, McMurry, PH., Formation and growth rates of ultrafine atmospheric particles: a review of observations, *J. Aerosol Sci.*, 35,143-176, 2004.

Kulmala, M., Petäjä, T., Nieminen, T., Sipilä, M., Manninen, H. E., Lehtipalo, K., Dal Maso, M., Aalto, P. P., Junninen, H., Paasonen, P., Riipinen, I., Lehtinen, K. E. J., Laaksonen, A., and Kerminen, V.-M.: Measurement of the nucleation of atmospheric aerosol particles, *Nat. Protoc.*, 7, 1651–1667, 2012.

Kulmala, M., Kontkanen, J., Junninen, H., Lehtipalo, K., Manninen, HE, Nieminen, T., Petaja, T., Sipila, M., Schobesberger, S., Rantala, P., Franchin, A, Jokinen, T., Jarvinen, E., Aijala, M., Kangasluoma, J., Hakala, J., Aalto, P. P., Paasonen, P., Mikkila, J., Vanhanen, J., Aalto, J., Hakola, H., Makkonen, U., Ruuskanen, T., Mauldin, R. L., III, Duplissy, J., Vehkamaki, H., Back, J., Kortelainen, A., Riipinen, I., Kurten, T., Johnston, M. V., Smith, J. N. Ehn, M., Mentel, T. F., Lehtinen, K. E. J., Laaksonen, A., Kerminen, V.-M. Worsnop, D. R., Direct Observations of Atmospheric Aerosol Nucleation, *Science,* 339, 943, 2013.

Formatted: English (US)

Formatted: English (US)

Formatted: Finnish

Formatted: Finnish

Kulmala, M., Petaja, T. Ehn, M., Thornton, J., Sipila, M., Worsnop, D. R., Kerminen, V. -M., Chemistry of Atmospheric Nucleation: On the Recent Advances on Precursor Characterization and Atmospheric Cluster Composition in Connection with Atmospheric New Particle Formation, *Annu. Rev. Phys. Chem*., 65, 21–37, 2014.

Kulmala, M., Luoma, K., Virkkula, A, Petaja, T., Paasonen, P., Kerminen, V.-M. Nie, W., Qi, X., Shen, Y., Chi, X., Ding, A., On the mode-segregated aerosol particle number concentration load: contributions of primary and secondary particles in Hyytiala and Nanjing *Boreal Environment Research*, 21, 319-331, 2016.

Leino, K., Nieminen, T., Manninen, H. E., Petaja, T., Kerminen, V.-M. and Kulmala, M., Intermediate ions as a strong indicator of new particle formation bursts in a boreal forest, BOREAL ENVIRONMENT RESEARCH, 21, 274-286, 2016.

Lelieveld J., Butler, T. M., Crowley, J. N., Dillon, T. J., Fischer, H., Ganzeveld, L., Harder, H., Lawrence, M. G., Martinez, M., Taraborrelli, D., Williams, J., Atmospheric oxidation capacity sustained by a tropical forest, *Nature* 452, 737-740, 2008.

Manninen, H. E., Nieminen, T., Asmi, E., Gagné, S., Häkkinen, S., Lehtipalo, K., Aalto, P., Vana, M., Mirme, A., Mirme, S., Hõrrak, U., Plass-Dülmer, C., Stange, G., Kiss, G., Hoffer, A., Törő, N., Moerman, M., Henzing, B., de Leeuw, G., Brinkenberg, M., Kouvarakis, G. N., Bougiatioti, A., Mihalopoulos, N., O'Dowd, C., Ceburnis, D., Arneth, A., Svenningsson, B., Swietlicki, E., Tarozzi, L., Decesari, S., Facchini, M. C., Birmili, W., Sonntag, A., Wiedensohler, A., Boulon, J., Sellegri, K., Laj, P., Gysel, M., Bukowiecki, N., Weingartner, E., Wehrle, G., Laaksonen, A., Hamed, A., Joutsensaari, J., Petäjä, T., Kerminen, V.-M., and Kulmala, M.: EUCAARI ion spectrometer measurements at 12 European sites – analysis of new particle formation events, *Atmos. Chem. Phys.*, 10, 7907-7927, doi:10.5194/acp-10-7907-2010, 2010.

Manninen, H. E., Mirme, S., Mirme, A., Petäjä, T., and Kulmala, M.: How to reliably detect molecular clusters and nucleation mode particles with Neutral cluster and Air Ion Spectrometer (NAIS), *Atmos. Meas. Tech.*, 9, 3577-3605, doi:10.5194/amt-9-3577-2016, 2016.

Martin, S. T., Andreae, M. O., Artaxo, P., Baumgardner, D., Chen, Q., Goldstein, A. H., Guenther, A., Heald, C. L., Mayol-Bracero, O. L., McMurry, P. H., Pauliquevis, T., Poeschl, U., Prather, K. A., Roberts, G. C., Saleska, S. R., Silva Dias, M. A., Spracklen, D. V., Swietlicki, E., Trebs, I., SOURCES AND PROPERTIES OF AMAZONIAN AEROSOL PARTICLES, REVIEWS OF GEOPHYSICS, 48, RG2002, DOI: 10.1029/2008RG000280, 2010a.

Martin, S. T., Andreae, M. O., Althausen, D., Artaxo, P., Baars, H., Borrmann, S., Chen, Q., Farmer, D. K., Guenther, A., Gunther, S. S., Jimenez, J. L., Karl, T., Longo, K., Manzi, A., Müller, T., Pauliquevis, T., Petters, M. D., Prenni, A. J., Pöschl, U., Rizzo, L. V., Schneider, J., Smith, J. N., Swietlicki, E., Tota, J., Wang, J., Wiedensohler, A., and Zorn, S. R.: An overview of the Amazonian Aerosol Characterization Experiment 2008 (AMAZE-08), *Atmos. Chem. Phys*., 10, 11415–11438, doi:10.5194/acp-10-11415-2010, 2010b.

Martin, S. T., Artaxo, P., Machado, L. A. T., Manzi, A. O., Souza, R. A. F., Schumacher, C., Wang, J., Andreae, M. O., Barbosa, H. M. J., Fan, J., Fisch, G., Goldstein, A. H., Guenther, A., Jimenez, J. L., Pöschl, U., Silva Dias, M. A., Smith, J. N., and Wendisch, M.: Introduction: Observations and Modeling of the Green Ocean Amazon (GoAmazon2014/5), *Atmos. Chem. Phys.*, 16, 4785-4797, doi:10.5194/acp-16-4785-2016, 2016.

S. T. Martin, P. Artaxo, L. Machado, A. O. Manzi, R. A. F. Souza, C. Schumacher, J. Wang, T. Biscaro, J. Brito, A. Calheiros, K. Jardine, A. Medeiros, B. Portela, S. S. de Sá, K. Adachi, A. C. Aiken, R. Albrecht, L. Alexander, M. O. Andreae, H. M. J. Barbosa, P. Buseck, D. Chand, J. M. Comstock, D. A. Day, M. Dubey, J. Fan, J. Fast, G. Fisch, E. Fortner, S. Giangrande, M. Gilles, A. H. Goldstein, A. Guenther, J. Hubbe, M. Jensen, J. L. Jimenez, F. N. Keutsch, S. Kim, C. Kuang, A. Laskin, K. McKinney, F. Mei, M. Miller, R. Nascimento, T. Pauliquevis, M. Pekour, J. Peres, T. Petäjä, C. Pöhlker, U. Pöschl, L. Rizzo, B. Schmid, J. E. Shilling, M. A. Silva Dias, J. N. Smith, J. M. Tomlinson, J. Tóta, and M. Wendisch, The Green Ocean Amazon Experiment (GoAmazon2014/5) observes pollution affecting gases, aerosols, clouds and rainfall over the rain forest, *Bull. Am. Meteor. Soc.*, DOI:10.1175/BAMS-D-15-00221.1, 2017.

Mather, J. H. and Voyles, J. W.: The ARM Climate Research Facility: A review of structure and capabilities, *Bull. Am. Meteor. Soc.*, 94, 377–392, 2013.

McFiggans, G, Artaxo, P., Baltensperger, U., Coe, H., Facchini, M. C., Feingold, G., Fuzzi, S., Gysel, M., Laaksonen, A., Lohmann, U., Mentel, T. F., Murphy, D. M., O'Dowd, C. D., Snider, J. R.) and Weingartner, E., The effect of physical and chemical aerosol properties on warm cloud droplet activation, *Atmos. Chem. Phys,* 6, 2593-2649, 2006.

Merikanto, J., Spracklen, D. V., Mann, G. W., Pickering, S. J., and Carslaw, K. S.: Impact of nucleation on global CCN, *Atmos. Chem. Phys*., 9, 8601-8616, doi:10.5194/acp-9-8601-2009, 2009.

Nieminen, T., Yli-Juuti, T., Manninen, H. E., Petäjä, T., Kerminen, V.-M., and Kulmala, M.: Technical note: New particle formation event forecasts during PEGASOS–Zeppelin Northern mission 2013 in Hyytiälä, Finland, *Atmos. Chem. Phys.,* 15, 12385-12396, doi:10.5194/acp-15-12385-2015, 2015.

Nieminen, T., Lehtinen, K. E. J. and Kulmala, M., Sub-10 nm particle growth by vapor condensation - effects of vapor molecule size and particle thermal speed, *Atmos. Chem. Phys.*, 10, 9773-9779; DOI: 10.5194/acp-10-9773-2010, 2010.

Rissler, J. et al. (2006) Size distribution and hygroscopic properties of aerosol particles from dry-season biomass burning in Amazonia, ACP 6, 471-491.

Rose, C., Sellegri, K., Velarde, F., Moreno, I., Ramonet, M., Weinhold, K., Krejci, R. Ginot, P., Andrade, M., Wiedensohler, A. and Laj, P., Frequent nucleation events at the high altitude station of Chacaltaya (5240 m a.s.l.), Bolivia, ATMOSPHERIC ENVIRONMENT, 102, 18-29, DOI: 10.1016/j.atmosenv.2014.11.015, 2015.

Tammet, H., Hõrrak, U., and Kulmala, M.: Negatively charged nanoparticles produced by splashing of water, *Atmos. Chem. Phys.*, 9, 357-367, doi:10.5194/acp-9-357-2009, 2009.

Deleted:

Tröstl, J., Chuang, W. K., Gordon, H., Heinritzi M., Yan C., Molteni U., Ahlm L., Frege C., Bianchi F., Wagner R., Simon M., Lehtipalo K., Williamson C., Craven J. S., Duplissy J., Adamov A., Almeida J., Bernhammer A.-K., Breitenlechner M., Brilke S., Dias A., Ehrhart S., Flagan R. C., Franchin A., Fuchs C., Guida R., Gysel M., Hansel A., Hoyle C. R., Jokinen T., Junninen H., Kangasluoma J., Keskinen H., Kim J., Krapf M., Kürten A., Laaksonen A., Lawler M.,Leiminger M., Mathot S., Möhler O., Nieminen T., Onnela A., Petäjä T., Piel F. – M., Miettinen P., Rissanen M. P., Rondo L., Sarnela N., Schobesberger S., Sengupta K., Sipilä M., Smith J. N., Steiner G., Tomè A., Virtanen A., Wagner A.C., Weingartner E., Wimmer D., Winkler P. M., Ye P., Carslaw K. S., Curtius J., Dommen J., Kirkby J., Kulmala M., Riipinen I., Worsnop D.R., Donahue N. M. and Baltensperger U., The role of low-volatility organic compounds in initial particle growth in the atmosphere, *Nature*, 533, 527-531, doi:10.1038/nature18271, 2016.

Vanhanen, J., Mikkilä, J., Lehtipalo, K., Sipilä, M., Manninen, H. E., Siivola, E., Petäjä, T., and Kulmala, M.: Particle size magnifier for nano-CN detection. *Aerosol Sci. Technol.*, 45:533–542, 2011.

Suni, T., Kulmala, M., Hirsikko, A., Bergman, T., Laakso, L., Aalto, P. P., Leuning, R., Cleugh, H., Zegelin, S., Hughes, D., van Gorsel, E., Kitchen, M., Vana, M., Hõrrak, U., Mirme, S., Mirme, A., Sevanto, S., Twining, J., and Tadros, C.: Formation and characteristics of ions and charged aerosol particles in a native Australian Eucalypt forest, *Atmos. Chem. Phys*., 8, 129-139, doi:10.5194/acp-8-129-2008, 2008.

Svenningsson, B., Arneth, A., Hayward, S., Holst, T., Massling, A., Swietlicki, E., Hirsikko, A., Junninen, H., Riipinen, I., Vana, M., Dal Maso, M., Hussein, T., and Kulmala, M.: Aerosol particle formation events and analysis of high growth rates observed above a subarctic wetland-forest mosaic, Tellus, 60B, 353–364, 2008

Thalman, R., de Sá, S. S., Palm, B. B., Barbosa, H. M. J., Pöhlker, M. L., Alexander, M. L., Brito, J., Carbone, S., Castillo, P., Day, D. A., Kuang, C., Manzi, A., Ng, N. L., Sedlacek III, A. J., Souza, R., Springston, S., Watson, T., Pöhlker, C., Pöschl, U., Andreae, M. O., Artaxo, P., Jimenez, J. L., Martin, S. T., and Wang, J.: CCN activity and organic hygroscopicity of aerosols downwind of an urban region in central Amazonia: seasonal and diel variations and impact of anthropogenic emissions, Atmos. Chem. Phys., 17, 11779-11801, https://doi.org/10.5194/acp-17-11779-2017, 2017.

Vana M., Kulmala, M., Dal Maso M. and Hõrrak, U., Comparative study of nucleation mode aerosol particles and intermediate air ions formation events at three sites, *Journal of Geophysical Research*, VOL. 109, D17201, doi:10.1029/2003JD004413, 2004

Vana, M., Ehn, M., Petaja, T., Vuollekoski, H., Aalto, P., de Leeuw, G., Ceburnis, D., O'Dowd, C. D. and Kulmala, M. Characteristic features of air ions at Mace Head on the west coast of Ireland,
ATMOSPHERIC RESEARCH, 90, 278-286, DOI: 10.1016/j.atmosres.2008.04.007, 2008.

Formatted: Finnish

Vanhanen, J., Mikkilä, J., Lehtipalo, K., Sipilä, M., Manninen, H. E., Siivola, E., Petäjä, T. and Kulmala, M. (2011), Particle Size Magnifier for Nano-CN Detection, *Aerosol Science and Technology,* 45: 4, 533 — 542, DOI: 10.1080/02786826.2010.547889, 2011.

Wagner, R., Manninen, H. E., Franchin, A., Lehtipalo, K., Mirme, S., Steiner, G., Petäjä, T. and Kulmala, M.: On the accuracy of ion measurements using a Neutral cluster and Air Ion Spectrometer, *Boreal Environment Research*, 21, 230-241, 2016.

Wang J., Krejci R., Giangrande S., Kuang, C., Barbosa H. M. J., Brito J., Carbone S., Chi X., ComstockJ., Ditas F., Lavric J., Manninen H. E., Mei F., Moran-Zuloaga D., Pöhlker C., Pöhlker M. L., Saturno J., Schmid B., Souza R. A. F., Springston S. R., Tomlinson J. M., Toto T., Walter D., Wimmer D., Smith J. N., Kulmala M., Machado L.A. T., Artaxo P., Andreae M. O., Petäjä T. & Martin S. T., Amazon boundary layer aerosol concentration sustained by vertical transport during rainfall, *Nature*, doi:10.1038/nature19819, 2016.

Wang, M. and Penner, J. E.' Aerosol indirect forcing in a global model with particle nucleation, *Atmos. Chem. Phys*., 9:1, 239-260, 2009.

Yu, F. and Luo, G.' Simulation of particle size distribution with a global aerosol model: contribution of nucleation to aerosol and CCN number concentrations, *Atmos. Chem. Phys.*, 9: 20, 7691-7710, 2009.

Tables

Deleted:

Table 1. A comparison between the sites during wet and dry season. Outside canopy site values on the left, inside canopy on the right. The months chosen for the wet season for inside the canopy are Jan-Mar and Dec-Mar for inside the canopy. Dry season includes Aug-Oct and July-Sept for outside and inside canopy. Aerosol and ion parameters from the NAIS measurements listed are ion concentrations in three size bins (0.8-2, 2-4 and 4-20 nm). Neutral particle concentrations in two different size bins from the NAIS (2-4 and 4-20 nm) and total particle concentrations (>10 nm) from CPC measurements and condensation sink from the SMPS. The numbers present diel medians and in brackets 25^{th}-75^{th} percentiles. Environmental parameters are temperature, relative humidity, precipitation, wind direction.

	Pasture site (T3)		Inside rainforest (T0t)	
Particle and ion concentrations				
	Wet	*Dry*	*Wet*	*Dry*
Cluster ions (0.8-2 nm) [cm^{-3}]	1000 (-) (836-1500)	988 (-) (688-1400)	814 (-) (641-1051) 968(+) (790-1178)	605(-) (465-801) 765(+) (604-1003)
Intermediate ions (2-4 nm) [cm^{-3}]	7 (-) (3-14)	8 (-) (4-16)	5(-) (2-10) 11(+) (7-17)	4(-) (2-8) 11(+) (7-16)
Large ions (4-20 nm) [cm^{-3}]	58 (-) (27-107)	56 (-) (30-106)	84(-) (40-178) 147(+) (62-410)	132(-) (52-425) 162 (80-329)
Intermediate particles (2-4 nm) [cm^{-3}]	579 (286-943)	550 (276-927)	477 (252-810)	591 (323-1003)
Large particles (4-20 nm) [cm^{-3}]	1000 (547-2150)	922 (552-1600)	308 (169-690)	530(-) (250-1070)
CPC total particles (>10 nm) [cm^{-3}]	1000 (533-1352)	731 (411-2000)	-	-
SMPS condensation sink [s^{-1}]	1.6 e-3 (9.5e-4-2.4e-3)	3.8 e-3 (2.3e-3-6.1e-3)	-	-
Environmental parameters				
Temp [°C]	25.7 (24.4 – 28.5)	26.1 (24.5 – 29.5)	24 (23-25)	24 (23-26)
RH [%]	94.8 (79.6 – 98.8)	92.8 (78.1 – 97.4)	97 (93-98)	96 (90-98)
Precipitation rate [mm hr^{-1}]	0 (0-0.15)	0 (0-0.16)	1.5 (0-6.5)	0.4 (0-3.9)
Total average precipitation [mm]	6.3 (5.6-13)	3.2 (0.3-13.6)	7.5 (3.4-30)	6.5 (2.3-13.9)
Wind direction [°; relative to north]	86.7 (40.85 - 156)	107.6 (38 - 224)	97 (58-143)	97 (60-147)
Wind speed [m s^{-1}]	1.5 (0.7 – 2.6)	1.1 (0.5 – 2.2)		

Deleted: Outside canopy

Deleted: canopy

Table 2. Annual statistics for ion and total particle concentration in T0t inside canopy site for the period of 2011-2014. Values represent median (25^{th}-75^{th} percentiles).

Size bin	Negative ion	Positive ions	Total particles
0.8-2 nm	723 (537-1012)	879 (683-1124)	-
2-4 nm	5 (2-9)	10 (7-16)	521 (278-889)
4-20 nm	85 (40-182)	151 (68-382)	380 (192-872)

Table 3. New particle formation (NPF) characteristics at the outside canopy (T3) site. Classified NPF event and rain-induced ion event frequencies.

	NPF days	Undefined	Non-events	Rain events	No-rain events
Wet season (Jan-Mar)	8/64 (12.5%)	0/64 (0%)	57/64 (89%)	61/64 (95%)	04/64 (6%)
Dry season (Aug-Oct)	0/46 (0%)	0/46 (0%)	46/46 (100%)	15/46 (32.6%)	34/46 (74%)

Deleted: 5
Deleted: 65
Deleted: 5
Deleted: 5
Deleted: 8
Deleted: 5
Deleted: 4
Deleted: 9
Deleted: 9
Deleted: 9
Deleted: 9
Deleted: 9
Deleted: 1
Deleted: 9
Deleted: 69

Table 4. The parameters shown are from the outside canopy site for nucleation/no nucleation event days. Median total particle concentration measured by a CPC, measured by the NAIS in two size ranges (2-4 and 4-20 nm) and negative ion concentrations from the NAIS in three size ranges (0.8-2, 2-4 and 4-20). The median values are calculated for the time window 09:00 – 12:00 as this is the time window of NPF events. The numbers in the brackets represent the 25th and 75th percentile. The second part of the table includes median numbers of environmental parameters for the whole day: temperature, RH, Precipitation and wind direction for NPF /no NPF days. The main differences are the condensation sink and the wind direction.

Particle and ion concentrations- 09:00 – 12:00 LT		
	NPF day	**Non NPF day**
Cluster ions (0.8-2 nm) [cm^{-3}]	800 (-) (692-905)	870 (-) (687-1000)
Intermediate ions (2-4 nm) [cm^{-3}]	13 (-) (6-23)	8 (-) (4-15)
Large ions (4-20 nm) [cm^{-3}]	83 (-) (44-137)	62 (-) (25-119)
Intermediate particles (2-4 nm) [cm^{-3}]	606 (303-969)	547 (522-1600)
Large particles (4-20 nm) [cm^{-3}]	1000 (604-1600)	970 (238-1000)
Full day data		
SMPS Condensation sink [s^{-1}]	1.6e-3 (8.4e-4-2.6e-3)	3.3e-3 (1.7e-3-5.5e-3)
CPC total particles (>10 nm) [cm^{-3}]	1100 (579-1860)	1000 (404-2000)
Environmental parameters-full day		
	NPF day	**Non NPF day**
Temp [°C]	25.6 (23.8 – 28.9)	26 (24.5 – 29.3)
RH [%]	94.2 (78.8 – 98.1)	93.5 (78.9 – 97.6)
Precipitation rate [mm hr^{-1}]	0 (0 - 0)	0 (0 – 0.16)
Total average precipitation [mm day^{-1}]	6.9 (5.8-8.2)	5.6 (0.9-15.3)
Wind direction [°; relative to north]	83 (56.95 – 120.8)	105.5 (38.8 – 217)
Wind speed [m s^{-1}]	1.85 (0.96 – 3.04)	1.2 (0.6 – 2.3)

Formatted: Superscript

Table 5. Growth rates (GR, nmh^{-1}) and nucleation rates (J; cm^{-3}s^{-1}) determined from the NAIS ion and particle data for each nucleation event. Also the median values for the condensation sink (CS; s^{-1}) for each event day are shown. The condensation sink is calculated from the SMPS size distributions. The GR were determined by finding the maximum concentration for different size bins for 2-3 nm, 3-7nm and 7-20 nm. The GR values present median values of the GR for positive and negative ions. The nucleation rates represent median numbers for positive and negative ions.

Deleted: The GR between ions and particles agree well with each other for the individual nucleation events. GR are smaller for the smaller size ranges and increase with particle size. The nucleation rates are in general higher for the particles than the ions. The Condensation is calculated from the SMPS size distributions.

Size bins	**2-3 nm**				**3-7 nm**				**7-20 nm**		
	Particles		*ions*		*Particles*		*Ions*		*Particles*		
	GR **(nm h^{-1})**	**J** (cm^{-3}s^{-1})	**GR** (nm h^{-1})	**J** (cm^{-3}s^{-1})	**GR** (nm h^{-1})	**J** (cm^{-3}s^{-1})	**GR** (nm h^{-1})	**J** (cm^{-3}s^{-1})	**GR** (nm h^{-1})	**J** (cm^{-3}s^{-1})	**CS** (s^{-1})
29.01.2014	0.8	0.19	1.4	0.003	2.8	0.097	1.7	0.001	-	-	-
30.01.2014	-	-	3.7	0.011	13.6	-	7.1	0.13	4.4	0.38	0.00076
06.02.2014	0.8	-	19.8	0.07	29	0.87	11	0.01	24	0.28	0.0016
12.02.2014	0.7	0.17	1.2	0.005	1.3	0.09	1.2	0.003	3	0.09	0.0016
12.03.2014	1.1	0.2	1.7	0.002	13.3	-	11.2	0.008	4.9	-	0.0014
13.03.2014	1.5	0.2	1.6	-	1.2	-	8	-	13.6	0.24	0.0015
18.03.2014	-	-	0.7	0.002	-	-	7.7	0.009	-	-	0.0017
25.03.2014	0.8	0.11	-	-	15.7	0.4	15.8	0.018	14	0.18	0.0017

Figures

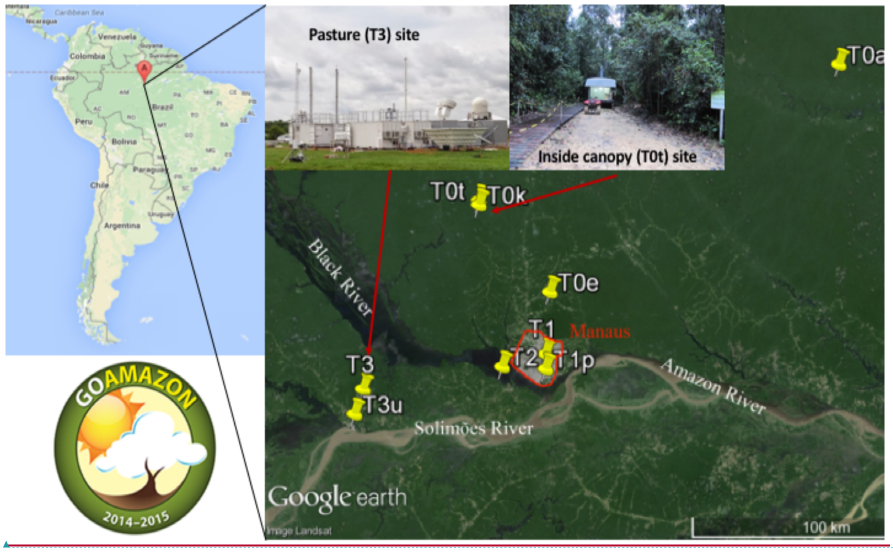

Figure 1. Location on map and photos of the inside canopy (T0t) and outside canopy (T3) sampling sites in Amazonas. The left column shows a map of South America and the right side shows a satellite view and photos of the T0t and T3 environment. From the inside canopy site we present the long term data, whereas from the outside canopy site we show the comparison of wet and dry season. The inside rainforest measurements at T0t is located in a pristine area, whereas the outside canopy site is located at T3, downwind of Manaus.

Formatted: Font:Bold

Deleted: canopy

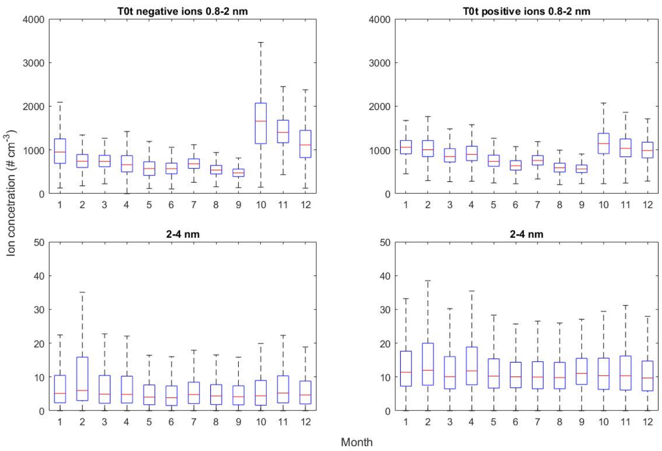

Figure 2. Annual variation of the negative (left column) and positive (right column) ion concentrations for 2011–2014 from inside the rainforest canopy. The bars represent median monthly ion concentrations, and the whiskers represent 25th and 75th percentiles.

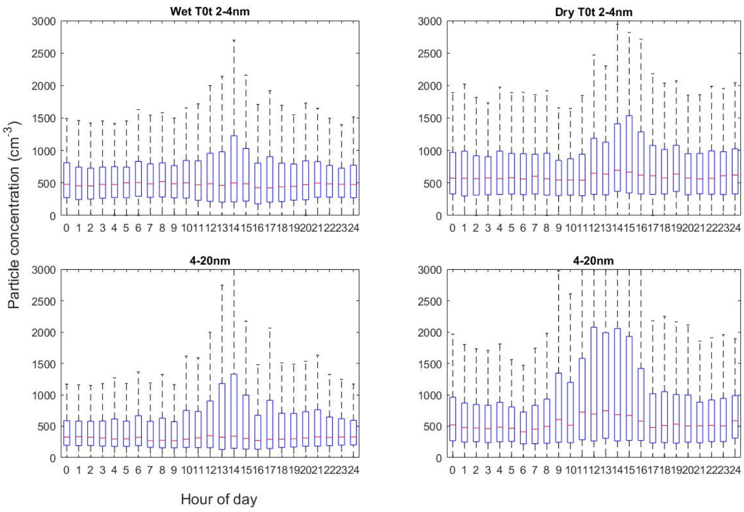

Figure 3. Diel cycle of total particle concentration at the inside canopy site (T0t) during the wet (Dec-Mar; left) and dry (Apr-Oct; right) season, for 2-4 nm (top) and 4-20 nm (bottom) particles.

Formatted: Font:

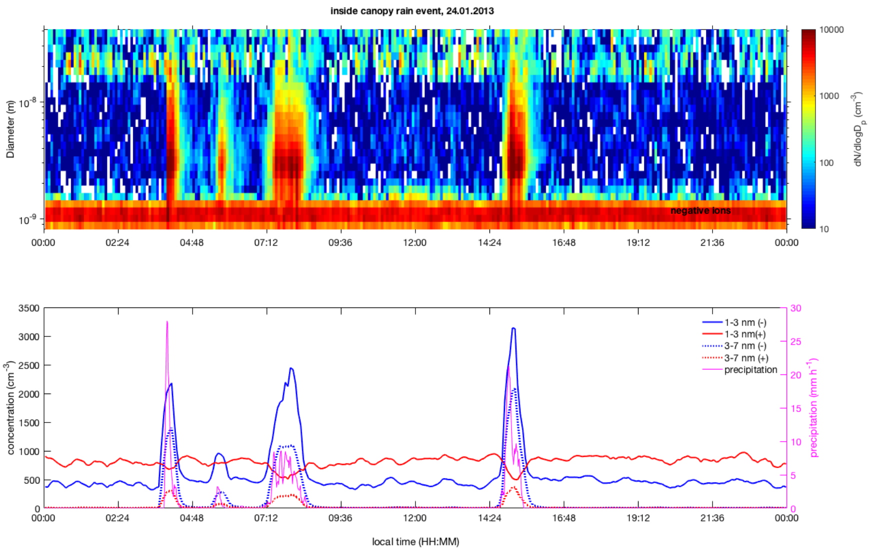

Figure 4. Typical rain-induced event at the inside canopy (T0t) site (Jan 24, 2013). Upper panel: negative ion number size distribution during a selected rain-induced ion production day measured with the NAIS. Lower panel: precipitation in mm h^{-1} (pink trace) on the right axis, concentration of small (1-3 nm) negative (blue) and positive (red) ions with the scale on the left axis.

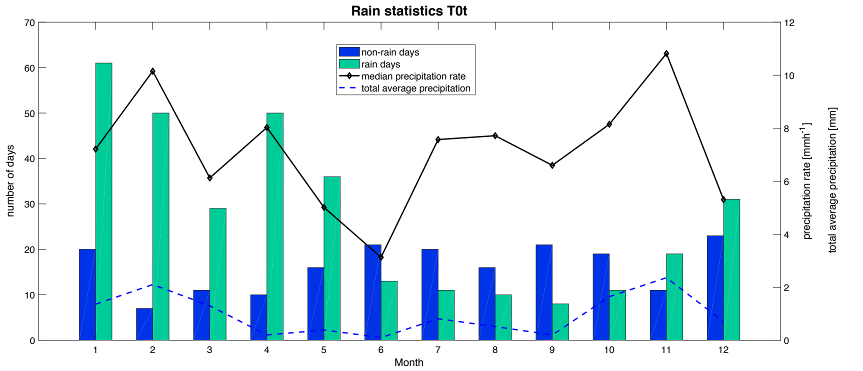

Figure 5. Inside canopy site (T0t) number of days with rain (green bars), no rain (red bars). On the right hand axis median precipitation rates (dashed blue line) and total average rain (solid black line).

Deleted: monthly

Deleted: frequencies (% of days with available data) of rain-induced ion events (n=306) and no-rain days (n=195). Dashed line indicates the median monthly variation of rain intensity (mm h^{-1}). Data collected continuously from September 2011 to January 2014 at the T0t site.

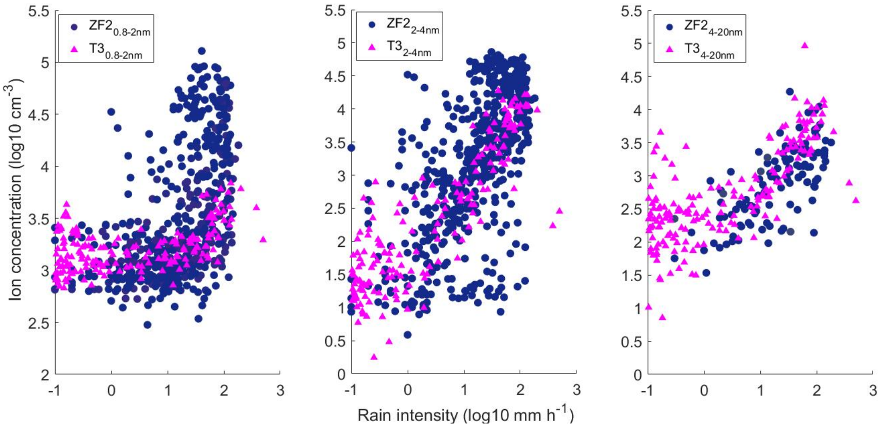

Figure 6. Median daily ion concentrations as a function of rain intensity at the inside canopy site (T0t) between September 2011 and January 2014 (blue circles). Outside canopy site (T3) rain events concentrations are added for comparison (triangles). (A) Cluster ions (0.8-2 nm), (B) 2-4 nm, and (C) 4-20 nm.

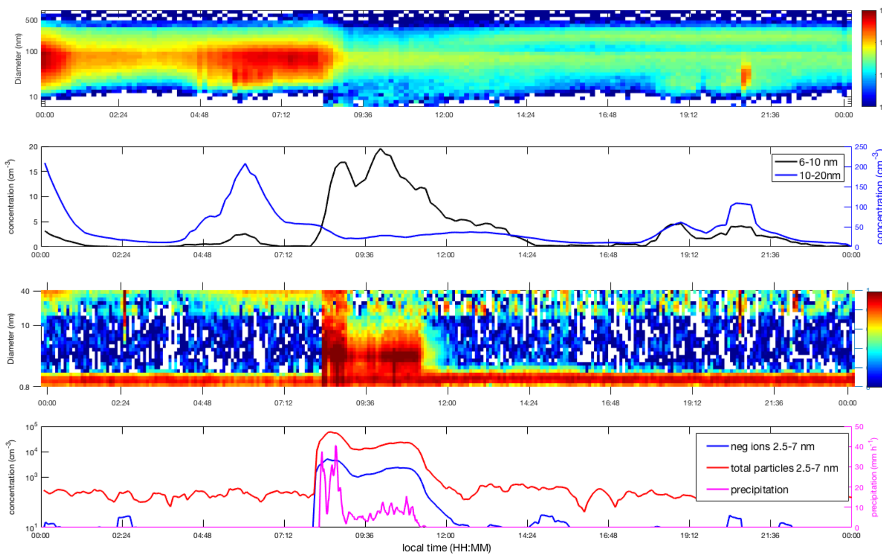

Figure 7. Example for a rain-induced event for total particles (DMPS). The DMPS measurements are taken above the canopy (60 m height), NAIS measurements are inside the canopy. Panel (a) shows the DMPS surface Figure. Panel (b) shows the particles measured by the DMPS for 6-10 nm (black line, left hand axis) and 10-20 nm (blue line, right hand axis). Panel (c) shows the surface Figure for the negative ions, measured by the NAIS. Panel (d) shows the negative ion concentrations for 2.5-7 nm in blue and the total particle concentration in the same size range from the NAIS in red with the scale on the left axis. The pink trace shows the precipitation in mm h^{-1} on the right axis.

Deleted: dashed line

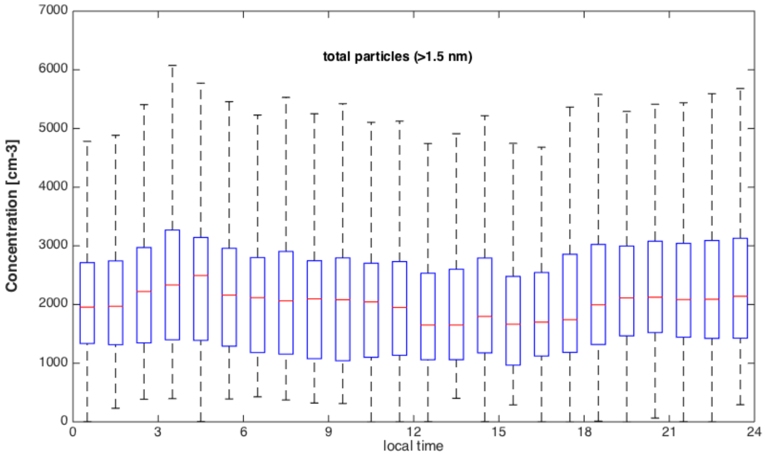

Fig 8. Diel cycle of particles bigger than 1.5 nm measured by the PSM during the dry season outside the rainforest canopy. In total, 38 days of data were used. The data shows hourly median concentrations, the whiskers 25th and 75th percentile.

Figure 9. Diel cycle of ions measured outside the canopy by the NAIS (small: 0.8–2 nm; intermediate: 2–4 nm; The lowest two panels show the total particles (large: 4–20 nm) from the NAIS and total particles >10 nm as measured by the MAOS CPC. The left column shows the NPF event days and the right column the non NPF days. The markers are hourly median number concentrations and the whiskers 25th and 75th percentiles.

Deleted: aerosol particles and

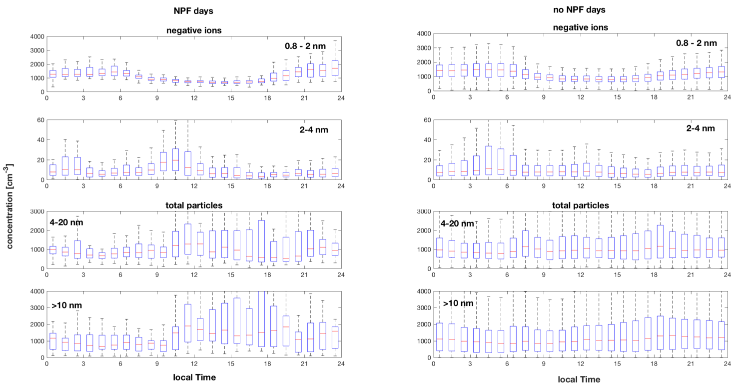

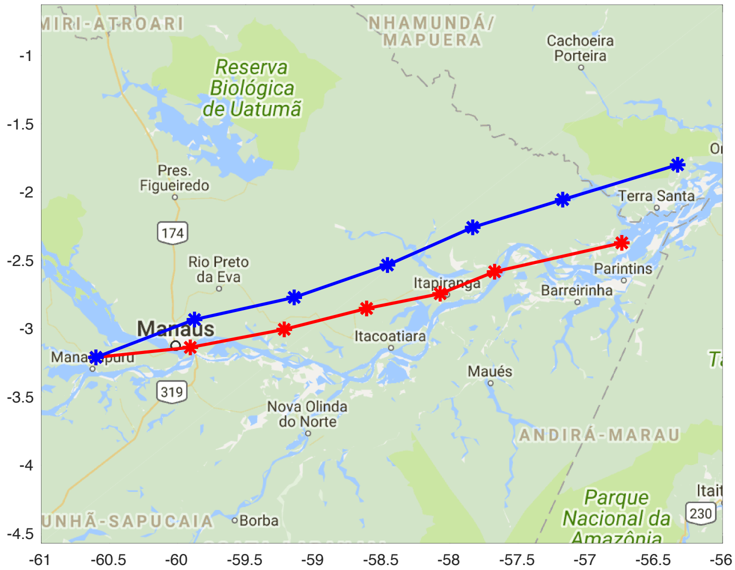

Figure 10: median back trajectories for NPF (blue) and non NPF (red) days. The trajectories were calculated 24hours backwards arriving at 09:00 local time at 500m a.s.l. at the measurement site.

Formatted: Font:

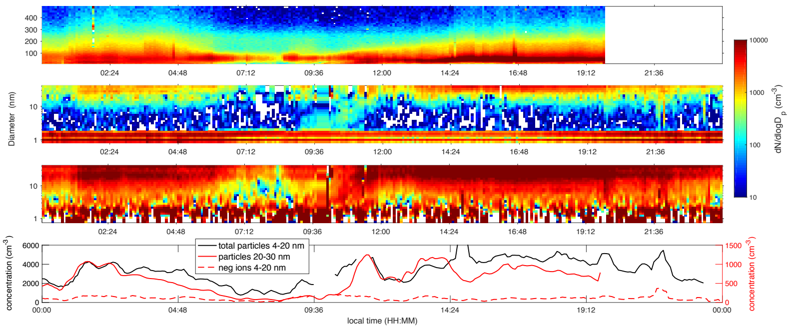

Figure 11 One example NPF day as observed at the outside canopy (T3) site. (a) shows the surface Figure from the SMPS, (b) and (c) show the surface Figures from the NAIS, (b) for negative ions, (c) for total particles. The color code indicates the measured concentrations. Panel (d) shows concentrations for the 20-30nm size range from the SMPS (black line) and from the NAIS the negative ion (dashed red line) and total particle concentrations (solid red line) in the 4-20 nm size range.

Formatted: Font:

Deleted: and

Deleted: a

Deleted: b

Deleted: c

Deleted: the mode diameter as measured by the MAOS SMPS. The mode diameter decreases at the start of the NPF event followed by continuous growth up to about 60 nm. Panel (d) shows negative ion and neutral particle concentrations in two size ranges (2-4 nm and 4-20 nm). Note the left axis is for the 2-4 nm ion concentration and 2-4 nm particle concentrations, right 4-20 neutral particle and ion concentrations.